UCRL-53119, Rev. 1

Mathematical Modeling of Modified *In Situ* and Aboveground Oil Shale Retorting

Robert L. Braun

January 1981

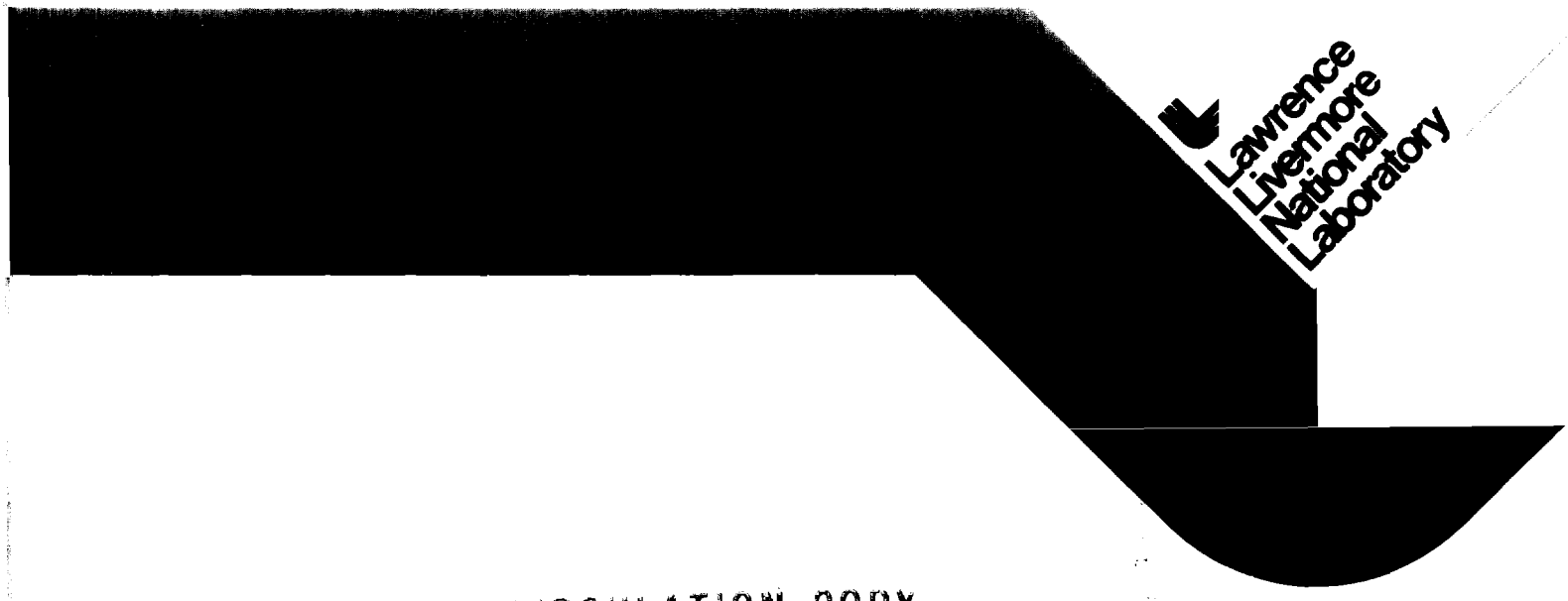

DISCLAIMER

Work performed under the auspices of the U.S. Department of Energy by Lawrence Livermore National Laboratory under Contract W-7405-Eng-48.

UCRL-53119, Rev. 1
Distribution Category UC-123

Mathematical Modeling of Modified *In Situ* and Aboveground Oil Shale Retorting

Robert L. Braun

Manuscript date: January 1981

LAWRENCE LIVERMORE LABORATORY
University of California • Livermore, California • 94550

CONTENTS

NOMENCLATURE

C = Heat capacity of shale (J/kg·K)

C_g = Heat capacity of gas (J/kg·K)

C_{O_2} = Oxygen concentration in bulk-gas stream (kg/m^3)

C_{H_2O} = Steam concentration in bulk-gas stream (kg/m)

D_{e,O_2} = Effective diffusivity of oxygen (m^2/s)

D_{e,H_2O} = Effective diffusivity of steam (m^2/s)

D_R = Diameter of retort (m)

D_W = Thickness of wall of retort (m)

f = Mass stoichiometry factors

$F(t)$ = Time-dependent function for input-gas temperature (K)

G_i = Superficial mass flux ($kg/m^2 \cdot s$)

H_i = Heat of reaction (J/kg)

h = Gas-solid heat transfer coefficient ($J/m^2 \cdot K \cdot s$)

k_d = Gas-solid mass transfer coefficient (m/s)

k_e = Effective axial thermal conductivity of bed ($J/m \cdot K \cdot s$)

k_1 = Rate coefficient for kerogen pyrolysis (s^{-1})

k_2 = Rate coefficient for $MgCO_3$ decomposition (s^{-1})

k_3 = Rate coefficient for $CaCO_3$ decomposition (s^{-1})

k_5 = Rate coefficient for char pyrolysis (s^{-1})

k_6 = Rate coefficient for C + CO_2 reaction (s^{-1})

k_7 = Rate coefficient for C + H_2O reaction ($s^{-1}Pa^{-1/2}$ or $S^{-1}Pa^{-1}$)

k_8 = Rate coefficient for C + O_2 reaction ($s^{-1}Pa^{-1}$)

k_{17} = Rate coefficient for oil vapor cracking (s^{-1})

K_1 = Equilibrium constant for water-gas shift reaction

K_2 = Equilibrium constant for oxygen exchange reaction on carbon

M_i = Molecular weights of gases (kg/mol)

N_j = Number of zones in shale particle

N_p = Number of particle size classes

N_z = Number of axial grid points

P_{CO} = Partial pressure of CO within shale particle (Pa)

P_{CO_2} = Partial pressure of CO_2 within shale particle (Pa)

P_{H_2O} = Partial pressure of H_2O in bulk-gas stream (Pa)

$\hat{P}_{H_2O}$ = Vapor pressure of H_2O (Pa)

P_{O_2} = Partial pressure of O_2 in bulk-gas stream (Pa)

P_0 = Average gas pressure in retort (Pa)

Q_g = Heat source term for gas ($J/m^3 bed \cdot s$)

Q_j = Heat source term for shale ($J/m^3 shale \cdot s$)

R = Gas constant (8.3143 $J/mol \cdot K$)

R_i = Rate of reaction ($kg/m^3 shale \cdot s$ or $kg/m^2 bed \cdot s$)

R_T = Heating rate in shale particle (K/s)

r_j = Spherical radius of shale particle in size class j (m)

t = Time (s)

T_g = Temperature of gas (K)

T_j = Temperature of shale (K)

T_{lj} = Surface temperature of shale (K)

T_H = Temperature at which release of bound water is completed (K)

T_L = Temperature at which release of bound water begins (K)

T_W = Temperature of exterior wall of retort (K)

U_i = Concentrations of shale components ($kg/m^3 shale$)

U_i^o = Initial concentrations of shale components ($kg/m^3 shale$)

X_{H_2O} = Mole fraction steam in bulk-gas stream

z = Axial distance in retort (m)

z_{max} = Length of retort (m)

α = Packing fraction of shale ($m^3 shale/m^3 bed$)

Δt = Finite-difference time interval (s)

Δz = Finite-difference axial increment (m)

ε = Porosity of bed ($m^3 void/m^3 bed$)

ε_k = Intraparticle porosity due to complete removal of kerogen

λ = Thermal conductivity of shale ($J/m \cdot K \cdot s$)

λ_W = Thermal conductivity of retort wall ($J/m \cdot K \cdot s$)

μ = Viscosity of bulk-gas stream ($kg/m \cdot s$)

ρ = Density of shale ($kg/m^3 shale$)

ρ_g = Density of gas ($kg/m^3 gas$)

τ = Residence time of gas in Δz (s)

MATHEMATICAL MODELING OF MODIFIED *IN SITU* AND ABOVEGROUND OIL SHALE RETORTING

ABSTRACT

A one-dimensional mathematical model has been developed for simulating the chemicophysical processes involved in the vertical retorting of a rubblized bed of oil shale. Included in the present model are those processes believed to have the most important effects in either the hot-gas retorting mode or the forward combustion mode. The physical processes are axial convective transport of heat and mass, axial thermal dispersion, gas-solid heat transfer, intraparticle shale thermal conductivity, water vaporization and condensation, wall heat loss, and movement of shale countercurrent to the flow of gas. The chemical reactions within the shale particles are release of bound water, pyrolysis of kerogen, coking of oil, pyrolysis of char, decomposition of carbonate minerals, and gasification of residual organic carbon with CO_2, H_2O, and O_2. The chemical reactions in the bulk-gas stream are combustion and cracking of oil vapor, combustion of H_2, CH_4, CH_x, and CO, and the water-gas shift.

The governing equations for mass and energy balance are solved numerically by a semi-implicit, finite-difference method. The computer program is written in LRLTRAN (an extended version of FORTRAN) for use on a CDC-7600 or CRAY computer. The bulk-gas flow rate as well as the composition and temperature of both the gas stream and the shale particles are calculated as a function of time and location in the retort.

INTRODUCTION

The Lawrence Livermore National Laboratory (LLNL) is engaged in research and development of a modified *in situ* process (MIS) to obtain oil from oil shale (Lewis and Rothman,[1] Rothman[2]). In this process, a portion of the oil shale is removed by underground mining, and the remainder is rubblized and retorted in place by a forward combustion technique. Construction of the large, *in situ* retorts is time-consuming and expensive. Therefore, it is desirable to reach commercialization of the process with a minimum of

experimentation in the field. An important and relatively inexpensive tool to assist in accomplishing that goal is a mathematical model for simulating the chemical reactions and physical processes involved.

Process simulation models for oil shale retorting have been developed independently by several private corporations, in particular Mobil (Kondis et al.[3] and Johnson et al.[4]) and Occidental (McCarthy and Cha[5]). Because these models are proprietary, they are not available to the public. Various nonproprietary models (e.g., Fausett[6] and Nuttall[7]) have generally not been comprehensive enough. However, a global retorting model has been developed at the Laramie Energy Technology Center (Dockter and Harris[8]) and further modified at the University of Wyoming (George and Harris[9,10]). Unfortunately, that model used several arbitrarily adjusted factors in order to obtain agreement with data from the Laramie 150-ton retort. Therefore, successful application of the model to other operating conditions is uncertain.

A keystone of the LLNL Oil Shale Project is the development of a mathematical retort model based on fundamental kinetics and thermodynamics for all of the processes that are chosen for inclusion in the model. Bowman[11] first formulated a set of governing equations for oil shale retorting, but the numerical solution of those equations proved to be excessively time-consuming. Subsequent to Bowman's work, a more modest approach was taken at LLNL in developing a retort model. A preliminary progress report was published by Braun and Chin.[12] The model has undergone further development, as warranted by an increased understanding of retorting fundamentals.

DESCRIPTION OF MODEL

The LLNL retort model is a transient, one-dimensional description of a packed bed. Variable properties in the vertical (axial) direction are considered. Thus, the model is meant to simulate adiabatic laboratory retorts and *in situ* retorts that have been prepared with fairly uniform lateral distribution of shale particle sizes, void volume, and permeability. Although the model does address the phenomenon of wall heat loss, it is not strictly valid for retorts having appreciable wall heat loss, since the resulting effects of the lateral temperature gradients cannot be properly treated in a one-dimensional model.

The model's main role is to calculate (as a function of time and axial location in the retort) the flow rate of the bulk-gas stream and the composition and temperature of both the fluid stream and the shale particles. Ten independent variables (G_i, i = 1, 2, ... 10) are used to describe the mass superficial flow rates of N_2, O_2, CO_2, CO, H_2, CH_4, CH_x, H_2O, oil vapor, and liquid water, respectively. Six independent variables (U_i, i = 1, 2, ... 6) are used to describe the shale composition in terms of the volatilizable components: kerogen, mineral CO_2 from $MgCO_3$, mineral CO_2 from $CaCO_3$, bound water, residual organic hydrogen, and residual organic carbon, respectively.

A given shale particle size distribution is handled by grouping the distribution into several representative spherical particle sizes (usually three), and solving the governing mass and energy equations for each size group. Different initial properties of the shale bed (shale composition, particle size distribution, and bed void fraction) may be specified at each axial grid point in the retort. Such specifying is important in order to simulate the actual variations in shale properties that may be encountered in the field. In addition, movement of the shale countercurrent to the direction of inlet gas flow is permitted in order to simulate aboveground (moving bed) retorts. For the latter case, the inlet-shale temperature, composition, particle size, bed porosity and linear velocity may be specified as a function of time.

For both MIS and aboveground retorts, the temperature, composition, and flow rate of the inlet gas may be specified as a function of time. Such specifying is important in order to simulate (1) the changes in inlet-gas properties that may be needed during ignition of the retort and (2) the changes required to control the retort operations as the retorting front encounters marked variations in oil shale grade. Inlet gas is not only permitted at one end of the retort, but also at any intermediate specified locations, as used in certain aboveground retort processes. Liquid water may likewise be introduced at any inlet-gas location to enable simulation of intentional or unintentional water influx at the top or side of an MIS retort and intentional water addition to aboveground retorts. All or part of the dry offgas from the end of the retort may also be recycled into any inlet-gas location.

The present model includes those processes believed to have the most important effects in either the hot-gas retorting mode or the forward combustion

TABLE 1. Chemical reactions and physical processes included in retort model.

Chemical reactions in shale particles	
	Release of bound water
	Pyrolysis of kerogen and coking of oil
	Pyrolysis of char
	Decomposition of carbonate minerals
	Reaction of carbon with carbon dioxide
	Reaction of carbon with oxygen
	Reaction of carbon with water
Chemical reactions in gas stream	
	Combustion and cracking of oil
	Combustion of H_2, CH_4, CH_x, and CO
	Water-gas shift
Physical processes	
	Axial convective transport of heat and mass
	Axial thermal dispersion
	Heat transfer between gas stream and shale particles
	Thermal conduction within shale particles
	Water vaporization and condensation
	Movement of shale countercurrent to flow of gas
	Wall heat loss

retorting mode. Table 1 summarizes the chemical reactions and physical processes included in the retort model.

REACTION RATES

KEROGEN PYROLYSIS

Much work has been reported on the kinetics and mechanism of kerogen pyrolysis (Hubbard and Robinson,[13] Allred,[14] Cummins and Robinson,[15] Braun and Rothman,[16] Fausett,[6] and Campbell et al.[17]). The pyrolysis apparently involves one or more intermediates in generating the products: char, oil, and gas. However, Campbell[17] showed that the rate of oil generation can be well-represented by one first-order reaction. We assume that the

disapperance of kerogen also follows first-order kinetics, because we do not distinguish kerogen from the actual oil-precursor intermediates. We also use kerogen to mean both soluble and insoluble organic material in the oil shale. For Green River oil shale,[18] the kerogen concentration is 1.242 times the measured initial organic carbon concentration. The rate of kerogen decomposition is then

$$R_1 = k_1 U_1 \quad \{kg\ kerogen/m^3 shale \cdot s\}$$

where:

$$k_1 = 2.81 \times 10^{13} \exp(-26390/T) \quad \{s^{-1}\}$$
$$H_1 = -3.30 \times 10^5 \quad \{J/kg\ kerogen\}$$
$$f_1 = 0.1664 \quad \{kg\ residual\ organic\ carbon/kg\ kerogen\}$$
$$f_2 = 0.0045 \quad \{kg\ residual\ organic\ hydrogen/kg\ kerogen\}$$
$$f_3 = 0.6585 \quad \{kg\ oil/kg\ kerogen\}$$
$$f_4 = 0.0106 \quad \{kg\ CO/kg\ kerogen\}$$
$$f_5 = 0.0390 \quad \{kg\ CO_2/kg\ kerogen\}$$
$$f_6 = 0.0042 \quad \{kg\ H_2/kg\ kerogen\}$$
$$f_7 = 0.0189 \quad \{kg\ CH_4/kg\ kerogen\}$$
$$f_8 = 0.0601 \quad \{kg\ CH_x/kg\ kerogen\}$$
$$f_9 = 0.0378 \quad \{kg\ H_2O/kg\ kerogen\}\ .$$

The endothermic heat of reaction (H_1) was estimated by Carley.[19] Mass stoichiometry factors (f_1 through f_9) were estimated by Raley[20] from analyses of Anvil Points shale.[21] The CH_x component (f_8) includes the hydrocarbons not condensed at 0°C. The detailed composition and average molecular weight of 0.0466 kg/mol or CH_x were also deduced from these data by Raley.[20] Note that we do not deal with the production of H_2S or NH_3. For mass balance, however, these are included in the H_2O component (f_9).

The released H_2 and CH_4 (f_6 and f_7) include products from the "primary" pyrolysis of kerogen at 500°C as well as part of the H_2 and all of the CH_4 from the "secondary" pyrolysis of the carbonaceous residue (char) above 500°C as determined by Campbell et al.[22] The residual organic hydrogen (f_2) represents the rest of the H_2 to be evolved during the char

pyrolysis (see reaction rate R_5). The residual organic carbon (f_1) represents the organic carbon remaining after complete pyrolysis of both the kerogen and the char.

DECOMPOSITION OF CARBONATE MINERALS

Decomposition of carbonate minerals is considered important because of the large endothermic heat of reaction. Accurate treatment of carbonate decomposition is difficult because of the large number of carbonate minerals and the variability of their kinetics and reaction paths depending upon the local gas composition. Campbell[23] has studied these reactions in samples of powdered oil shale, and he has proposed a detailed scheme for modeling them. The present retort model has adopted a more simplified version. We consider only two mineral CO_2 components. The first component (U_2) represents CO_2 from the $MgCO_3$ portion of dolomite as well as the CO_2 from other relatively low-temperature decomposing carbonates, such as ferroan, nahcolite, and dawsonite. This is a valid representation only if the latter minerals are present in minor quantities. The other component (U_3) represents the CO_2 from the $CaCO_3$ portion of dolomite and from the initial calcite content. First-order reaction rate coefficients from Campbell's experiments[23] are used:

$$R_2 = k_2 U_2 \quad \{kg\ CO_2/m^3 shale \cdot s\}$$

and

$$R_3 = k_3 U_3 \quad \{kg\ CO_2/m^3 shale \cdot s\}$$

where:

$$k_2 = 1.7 \times 10^{10} \exp(-29090/T) \quad \{s^{-1}\}$$
$$H_2 = -3.0 \times 10^6 \quad \{J/kg\ CO_2\}$$
$$k_3 = 9.6 \times 10^{10} \exp(-36050/T) \quad \{s^{-1}\}$$
$$H_3 = -2.9 \times 10^6 \quad \{J/kg\ CO_2\}.$$

The value for k_3 is based on a local CO_2 pressure of 0.5 atm. The heats of reaction are calculated from the standard heats of formation for the following reactions:

$$MgCO_3 = MgO + CO_2$$

and

$$5CaCO_3 + 2SiO_2 = 2Ca_2SiO_4 + CaO + 5CO_2.$$

The actual stoichiometry of the $CaCO_3$ reaction, and therefore the heat of reaction, depends on the details of temperature and gas composition. In block experiments,[24] x-ray diffraction analyses revealed the presence of appreciable quantities of spurrite ($Ca_5Si_2O_8CO_3$) in samples that had been heated at 704°C long enough to react most of the $CaCO_3$. The spurrite continued to decompose more slowly, resulting in the final products shown in the preceding equation. Steam is known to increase the reaction rate and the extent of Ca and Mg silicate formation in powdered samples of oil shale.[25] However, modeling the carbonate reactions in blocks of oil shale[26] has been most successful using Campbell's nonsteam kinetics, even for block experiments using a sweep gas containing 40% steam, presumably because carbonates within a block are not in a steam environment.

RELEASE OF BOUND WATER

Raw shale typically contains 1 to 2 wt% of bound water from analcime, illite, and other minerals. This water is assumed to evolve linearly with increasing temperature, in the temperature range of T_L to T_H; i.e.,

$$R_4 = U_4^{\circ} R_T / (T_H - T_L) \quad \{kg\ H_2O/m^3 shale \cdot s\} \quad ,$$

where:

$$R_T = \frac{\partial T}{\partial t} \quad \{K/s\}$$

and

$$H_4 = -2.26 \times 10^6 \quad \{J/kg\ H_2O\} \ .$$

This is a close approximation of the measured release of bound water from blocks of oil shale,[27] with T_L = 393 K and T_H = 633 K.

RELEASE OF RESIDUAL ORGANIC HYDROGEN

In this reaction, the remaining H_2 is evolved from char pyrolysis. Campbell et al.[22] have studied the kinetics of H_2 evolution up to temperatures of 900°C. They asserted that since the char is a very heterogeneous mixture of organic compounds, it is probable that the H_2 emission occurs from a large number of chemically nonequivalent sites. Thus, to accurately simulate that emission, a distribution of activation energies should be used. However, for shale heating rates typically encountered in MIS retorting (~1°C/min), the broad evolution of H_2 from char pyrolysis can readily be modeled by using a single first-order reaction and a relatively low activation energy. That is,

$$R_5 = k_5 U_5 \quad \{kg\ H_2/m^3 shale \cdot s\},$$

where:

$$k_5 = 10.7 \exp(-10190/T) \quad \{s^{-1}\}.$$

The heat of reaction (H_5) is not known for this reaction, but is presumed to be small. Precautions must be exercised if this rate expression is applied at very low heating rates.

CARBON GASIFICATION REACTIONS

The organic carbon residue in spent shale may react with CO_2, H_2O, and O_2. While only the latter reaction is exothermic and directly furnishes process energy, the other two reactions are also important because they enhance the removal of the carbon residue and produce useful gaseous products,

CO and H_2. These products are, in part, burned in the retort to furnish additional process energy and, in part, evolved from the retort to contribute to the heating value of the offgas. In modeling these reactions, separate rate equations are developed for each reaction (R_6, R_7, and R_8, for CO_2, H_2O, and O_2, respectively). The net rate of carbon gasification is then the sum of these three individual rates. The general model for simultaneous reactions between one solid reactant in a porous solid and two or more fluid reactants is based upon the law of additive reaction times[28] and has been tested over wide-ranging conditions by Sohn and Braun.[29]

Reaction of Residual Organic Carbon with CO_2 ($C + CO_2 = 2\ CO$)

The gasification of residual organic carbon by reaction with CO_2 has been studied extensively in powder samples of spent oil shale by Burnham[30,31] and Thomson et al.[32] Comparison of the results of these two investigations showed[32] that Burnham's kinetics consistently predicted a rate approximately four times higher than Thomson's. Mathematical analysis of oil shale block experiments (Mallon and Braun,[24] Gregg, Campbell, and Taylor,[33] and Braun, Mallon, and Sohn[26]) has shown that kinetics approximately five to ten times lower than Burnham's must be used in order to get agreement in the amount of carbon reacted. The reasons for these discrepancies are not known. It seems most prudent to use the block analyses as a basis for the present overall retort model.

Thus, the rate of reaction can be expressed according to the Ergun[34] equation as

$$R_6 = \frac{k_6 U_6}{f_{13}\left[1 + \frac{P_{CO}}{K_2\ P_{CO_2}}\right]} \qquad \{kg\ CO_2/m^3 shale \cdot s\}$$

where:

$$k_6 = 5.7 \times 10^4 \exp(-20130/T) \quad \{s^{-1}\}$$
$$K_2 = 4.15 \times 10^3 \exp(-11420/T)$$
$$H_6 = -3.92 \times 10^6 \quad \{J/kg\ CO_2\}$$
$$f_{12} = 1.2729 \quad \{kg\ CO/kg\ CO_2\}$$
$$f_{13} = 0.2729 \quad \{kg\ C/kg\ CO_2\}.$$

The oxygen-exchange equilibrium coefficient on carbon (K_2) is taken from Ergun.[34] The rate coefficient (k_6) is taken from recent block analyses of Braun, Mallon, and Sohn,[26] and is very close to the coefficient successfully used by Mallon and Braun[24] in previous block analyses. Interestingly, that previous coefficient was based on measurements of Taylor and Bowen[35] for the reaction of CO_2 with chars produced from subbituminous coals. We will return to this point in discussing the reaction of carbon with H_2O.

The remaining problem in evaluating the equation for R_6 is the lack of knowledge of the intraparticle gas composition. Whereas in a model of an individual shale particle (block) it is feasible to expend the required computer memory and execution time to gain this knowledge, in an overall retort model of a large collection of shale particles this is not practical. Therefore, appoximations must be made. In the block model of Gregg et al.[33] the simple approximation was made that $P_{CO}/K_2P_{CO_2}$ was constant during the entire reaction. While this could be supported for the constant heating rate condition used in their work, it is not valid for the more general temperature history encountered in an actual retort. A better approximation is that the partial pressure of a given gas species is proportional to its rate of production. Thus, the partial pressure of CO is

$$P_{CO} \propto 2R_6$$

and the partial pressure of CO_2 is

$$P_{CO_2} \propto R_{CO_2} - R_6.$$

The rate of CO_2 production from carbonate decomposition is

$$R_{CO_2} = (R_2 + R_3)\ U_6/U_6^o\ .$$

The latter equation recognizes that the carbon gasification will, on the average, be occurring in the fraction of the shale particle defined by U_6/U_6^o. The use of these approximations results in a net gasification equation that can be quadratically solved for R_6.

This formulation should be valid when the CO_2 consumed in the carbon gasification reaction is predominantly derived from carbonate decomposition, but may not be valid when the retort inlet gas contains an appreciable amount of CO_2. In the latter event, diffusion of CO_2 from the bulk-gas stream into the shale particle may become important.

Reaction of Residual Organic Carbon with H_2O ($C + H_2O = CO + H_2$)

In this gasification reaction, we recognize the three possible rate limiting steps: the rate of mass transfer of H_2O from the bulk-gas stream to the surface of the shale particle (R_{7c}), the rate of diffusion of H_2O into the shale particle (R_{7b}), and the rate of chemical reaction between H_2O and C (R_{7a}). Thus, from the law of additive reaction times,[28] the net rate of reaction is

$$R_7 = \frac{1}{\frac{1}{R_{7a}} + \frac{1}{R_{7b}} + \frac{1}{R_{7c}}} \quad \{kg\ H_2O/m^3 shale \cdot s\} .$$

The heat of reaction and stoichiometry factors are

$$H_7 = -7.29 \times 10^6 \quad \{J/kg\ H_2O\}$$
$$f_{14} = 0. \quad \{kg\ CO_2/kg\ H_2O\}$$
$$f_{15} = 1.5548 \quad \{kg\ CO/kg\ H_2O\}$$
$$f_{16} = 0.1119 \quad \{kg\ H_2/kg\ H_2O\}$$
$$f_{17} = 0.6667 \quad \{kg\ C/kg\ H_2O\}.$$

The mass transfer rate is

$$R_{7c} = 3\ k_d\ C_{H_2O} / \left[r_j (1 + X_{H_2O}) \right] ,$$

where:

$$C_{H_2O} = P_{H_2O} M_3 / (RT) \quad \{kg\ H_2O/m^3 gas\}$$

and

$$P_{H_2O} = \left(\frac{G_8}{M_8}\right) P_0 \Big/ \sum_{i=1}^{8} \left(\frac{G_i}{M_i}\right) \qquad \{Pa\} \ .$$

The gas-solid mass transfer coefficient (k_d) is discussed in Appendix A.

The H_2O diffusion rate can be approximated by[28,36]

$$R_{7b} = \left[\frac{\ell n\left(1 + X_{H_2O}\right)}{X_{H_2O}}\right] \left(\frac{3\, D_{e,H_2O}\, C_{H_2O}}{r_j^{\,2}}\right) \left[\left(\frac{U_6^o}{U_6}\right)^{1/3} - 1\right]^{-1} ,$$

where:

$$X_{H_2O} = P_{H_2O}/P_0 \quad \{\text{mole fraction } H_2O\}$$

and

$$D_{e,H_2O} = 7.4 \times 10^{-16} \left(U_1^o\right)^2 T^{1.73} \quad \{m^2/s\} \ .$$

The effective diffusivity is discussed in Appendix A. The first factor in the above equation for R_{7b} is needed since the volume of the gas products of this reaction exceeds the volume of the gas reactant diffusing into the particle by a factor of 2. It should be noted that the effect of bulk flow of other gases, such as the transpiration of CO_2 from carbonate decomposition, is not addressed in the diffusion equations for either H_2O or O_2. More rigorous modeling of individual oil shale blocks[26] has indicated that neglecting the bulk flow effect on H_2O diffusion may not be serious for typical MIS retorting conditions. This aspect remains under investigation.

The chemical reaction rate (R_{7a}) is the final, and most uncertain, term to evaluate. The intrinsic chemical kinetics have been extensively studied by Burnham[37] and Thomson et al.[32] Again, Burnham's kinetics were appreciably higher than Thomson's. Neither set of kinetics gave accurate results when used in the analysis of block experiments, even when the Langmuir-Hinshelwood formulation was used to account for inhibition effects. Therefore, other kinetic formulations were considered for the retort model.

The most encouraging formulation is based on coal char data. Recall, from the discussion on the reaction of carbon with CO_2, that the chemical kinetics determined from analysis of oil shale block experiments were very close to the kinetics determined for subbituminous coal char. Because of that agreement, it was enticing to test the use of comparable data of Taylor and Bowen[35] for the rate of reaction of steam with subbituminous coal char; i.e.,

$$R_{7a} = k_7 \left(P_{H_2O}\right)^{1/2} U_6/f_{17},$$

where:

$$k_7 = 3.14 \times 10^3 \exp(-22140/T) \quad \{s^{-1}\ Pa^{-1/2}\}.$$

The reaction is reported to be first-order with respect to carbon[35] and approximately half-order with respect to H_2O.[37] This formulation of R_{7a} has been tested by comparison of model calculations with the data from many retort experiments and has shown more encouraging results than various alternatives.

One optional formulation of R_{7a}, based on the Langmuir-Hinshelwood equation, is permitted in the model:

$$R_{7a} = \left(\frac{k_7\ P_{H_2O}\ U_6}{1 + k_7'\ P_{H_2} + k_7''\ P_{H_2O}}\right)\left(\frac{U_6}{U_6^o}\right)$$

where:

$$k_7 = 9.87 \times 10^3 \exp(-28000/T) \quad \{s^{-1}\ Pa^{-1}\}$$
$$k_7' = 3.26 \times 10^{-4} \quad \{Pa^{-1}\}$$
$$k_7'' = 0.313 \exp(-10120/T) \quad \{Pa^{-1}\}\ .$$

Burnham[38] recommended the pseudo second-order reaction with respect to carbon. The adsorption coefficients, k_7' and k_7'', are taken from Long and Sykes,[39] and the rate coefficient, k_7, from Braun, Mallon, and Sohn.[26] This formulation has worked well in modeling individual blocks.

Reaction of Residual Organic Carbon with O_2 $(C + O_2 = CO_2)$

In this gasification reaction we again recognize the three possible rate limiting steps,

$$R_8 = \frac{1}{\frac{1}{R_{8a}} + \frac{1}{R_{8b}} + \frac{1}{R_{8c}}} \qquad \{\text{kg } O_2/m^3\text{shale}\cdot s\} .$$

The heat of reaction and stoichiometry factors are

$$H_8 = 1.23 \times 10^7 \quad \{J/\text{kg } O_2\}$$
$$f_{18} = 1.375 \quad \{\text{kg } CO_2/\text{kg } O_2\}$$
$$f_{19} = 0. \quad \{\text{kg CO/kg } O_2\}$$
$$f_{20} = 0.375 \quad \{\text{kg C/kg } O_2\}.$$

The mass transfer rate is

$$R_{8c} = 3k_d C_{O_2}/r_j \quad \{\text{kg } O_2/m^3\text{shale}\cdot s\}$$

where:

$$C_{O_2} = P_{O_2} M_2/(RT) \quad \{\text{kg } O_2/m^3\text{gas}\}$$

and

$$P_{O_2} = \left(\frac{G_2}{M_2}\right) P_0 \Big/ \sum_{i=1}^{8} \left(\frac{G_i}{M_i}\right) \quad \{Pa\}.$$

The O_2 diffusion rate can be approximated by[38]

$$R_{8b} = \left(\frac{3 D_{e,O_2} C_{O_2}}{r_j^2}\right) \left[\left(\frac{U_6^o}{U_6}\right)^{1/3} - 1\right]^{-1} \qquad \{\text{kg } O_2/m^3\text{shale}\cdot s\},$$

where:

$$D_{e,O_2} = 1.04 \times 10^{-15} \left(U_1^o\right)^2 T^{1.65} \quad \{m^2/s\} .$$

The effective diffusivity is discussed in Appendix A. The O_2 diffusion rate equation is somewhat simpler than the corresponding equation for H_2O because equimolar counterdiffusion is involved if the product of the reaction is CO_2.

The chemical reaction rate (R_{8a}) is relatively unimportant for this reaction, since it is so rapid. That is, diffusion of O_2 into the shale particles will be the rate-limiting step for most conditions that will be encountered in MIS retorting. This, of course, will not be the case in many aboveground retort processes, particularly processes using very small particle sizes (Lurgi and fluidized-bed processes). In simulating MIS retorting, the chemical reaction becomes the rate-limiting step only at temperatures near and below 400°C. Thus, it must be included in the equation in order to quench the reaction at the trailing edge of the thermal profile. Since the shale cooling rate is relatively rapid, little additional reaction occurs once the reaction becomes limited by the intrinsic chemical kinetics. Therefore the net reaction rate is very insensitive to the chemical kinetics. The retort model uses the following equation for the chemical reaction rate:

$$R_{8a} = k_8 P_{O_2} U_6 / f_{20} \quad \{kg\ O_2/m^3 shale \cdot s\} ,$$

where:

$$k_8 = 2.47 \exp(-11100/T) \quad \{s^{-1} Pa^{-1}\} .$$

The value used for k_8 is the intrinsic chemical reaction rate measured by Sohn and Kim.[40] Measurements by Thomson et al.[32] indicate a rate coefficient approximately a factor of 3 smaller than Sohn's coefficient. Fortunately, reduction in Sohn's rate coefficient by even a factor of 20 gives little effect in simulating MIS retorting. For fluidized-bed calculations, however, it will be important to know whether Sohn's or Thomson's chemical reaction rate coefficient is more accurate.

COKING OF OIL WITHIN SHALE PARTICLES

Thermal degradation (coking) of oil within blocks of oil shale has been investigated by Campbell et al.[27] The degree of coking depends strongly on the heating rate of the shale at the time of oil generation, but is nearly independent of particle size and grade for the conditions used. In shale particles up to 17 cm in diameter, the carbon residue produced by this reaction

was distributed uniformly within the particle for heating rates (R_T) ranging from 0.0005 to 0.05 K/s. Campbell proposed a detailed model that agreed with these observations. However, for the present study a simpler relationship was derived from Campbell's data for 17-cm particles. The rate of coking can be expressed as

$$R_9 = \frac{0.003635}{\sqrt{R_T}} f_3 R_1 \quad \{\text{kg oil/m}^3\text{shale}\cdot\text{s}\}.$$

The stoichiometry factors for the coking reaction, estimated by Raley,[20] are

$$f_{21} = 0.7038 \quad \{\text{kg C/kg oil}\}$$
$$f_{22} = 0.0604 \quad \{\text{kg } H_2\text{/kg oil}\}$$
$$f_{23} = 0.1927 \quad \{\text{kg } CH_4\text{/kg oil}\}$$
$$f_{24} = 0.0431 \quad \{\text{kg } H_2O\text{/kg oil}\}.$$

The heat of reaction is not known, but is presumed to be small.

CONDENSATION (OR VAPORIZATION) OF WATER

$$R_{10} = G_8 \left(1 - \frac{\hat{P}_{H_2O}}{P_{H_2O}}\right) \quad \{\text{kg } H_2O/\text{m}^2\cdot\text{s}\},$$

where

$\hat{P}_{H_2O}$ = {see Appendix A}
P_{H_2O} = {as defined for R_7}
$H_{10} = 2.26 \times 10^6$ {J/kg H_2O}.

WATER-GAS SHIFT ($CO + H_2O = CO_2 + H_2$)

Accurate calculation of the gas composition in a retort requires knowledge of the kinetics and equilibrium of the water-gas shift reaction (WGSR). The chemical equilibrium coefficient can, of course, be calculated as a function of temperature from the standard thermodynamic data. The kinetics, however, may be strongly influenced by the presence of metal oxide catalysts.

Therefore, the kinetics should be based on experimental measurements of this reaction as it occurs in the presence of oil shale.

Although experimental work has begun on this reaction by Thomson et al.[32] and Steward,[41] there appear to be major differences between these two investigations. The preliminary results of Steward, however, are at least qualitatively similar to the kinetics measured by Grebenshchikova[42] for the WGSR in the presence of ash from Lisichansk coal which has long been used as a basis for the WGSR in our retort model. Therefore, until more complete and consistent investigations are made for this reaction in the presence of oil shale, we will continue to use the coal ash kinetics.

Grebenshchikova[42] reported that the reaction was first-order with respect to CO up to concentrations of 65%. He did not study the reaction orders for the other three gases. Steward[41] estimated half-order for CO and zero order for H_2O, CO_2, and H_2, while Thomson[32] fit his data to first-order for all four gases with inhibition effects from CO_2 and H_2O. Because of these uncertainties and because the approach to equilibrium can be much more readily calculated using the first-order approximation, we fit the data of Grebenshchikova to first-order with respect to all four gases. Thus,

$$-\frac{dC_{H_2O}}{dt} = k_{11}\left(C_{CO}C_{H_2O} - \frac{1}{K_1}C_{CO_2}C_{H_2}\right) \quad \{mol/m^3 gas \cdot s\} .$$

In terms of the superficial mass fluxes (G_i), it is readily shown that the net rate of the WGSR as the gas stream moves an incremental distance (Δz) in the retort is implicitly given by

$$R_{11} = k'_{11}\left[(G_8 - R_{11})\left(\frac{G_4}{f_{27}} - R_{11}\right) - \frac{1}{K_1}\left(\frac{G_3}{f_{25}} + R_{11}\right)\left(\frac{G_5}{f_{26}} + R_{11}\right)\right] \{kg\ H_2O/m^2 \cdot s\}$$

where:

$$k'_{11} = \left(\frac{k_{11}\varepsilon\,\Delta z}{M_8}\right)\left[\left(\frac{P_0}{RT}\right)\Big/\sum_{i=1}^{8}\left(\frac{G_i}{M_i}\right)\right]^2 \quad \{m^2 \cdot s/kg\},$$

$k_{11} = 3.75 \times 10^2 \exp(-7300/T)$ $\{m^3 gas/mol \cdot s\}$

$K_1 = 1.7 \times 10^{-2} \exp(4400/T)$

$H_{11} = 2.29 \times 10^6$ $\{J/kg\ H_2O\}$

$f_{25} = 2.4429$ $\{kg\ CO_2/kg\ H_2O\}$

$f_{26} = 0.1119$ $\{kg\ H_2/kg\ H_2O\}$

$f_{27} = 1.5548$ $\{kg\ CO/kg\ H_2O\}$.

Note that R_{11} is a change in flux, not concentration. Upon completion of further experimental measurements of the WGSR in the presence of oil shale, the retort model will be modified accordingly.

COMBUSTION REACTIONS IN BULK-GAS STREAM

Specific reaction rate coefficients are not used for the combustion of H_2, CH_4, CH_x, CO, and oil in the bulk-gas stream. Rather, the combustion reactions are allowed to go to completion in each axial increment (Δz) of the retort and thereby completely consume either the fuel or the oxygen, whichever is limiting. Certain constraints imposed on this procedure will be discussed after presentation of the rate equations, heats of reaction, and stoichiometry factors. Note that for combustion of oil, CH_4, and CH_x the indicated reaction products are CO and H_2O, but provision is made for specifying other products. The indicated heat of reaction is consistent with the products being CO and H_2O and must be changed if a different set of products is specified.

Combustion of H_2

$$R_{12} \leq G_5/f_{29} \quad \{kg\ O_2/m^2 \cdot s\}$$

where:

$$H_{12} = 1.51 \times 10^7 \quad \{J/kg\ O_2\}$$
$$f_{28} = 1.126 \quad \{kg\ H_2O/kg\ O_2\}$$
$$f_{29} = 0.126 \quad \{kg\ H_2/kg\ O_2\}.$$

Combustion of CH_4

$$R_{13} \leq G_6/f_{32} \quad \{kg\ O_2/m^2 \cdot s\}$$

where:

$$H_{13} = 1.08 \times 10^{-7} \quad \{J/kg\ O_2\}$$
$$f_{30} = 0. \quad \{kg\ CO_2/kg\ O_2\}$$
$$f_{31} = 0.750 \quad \{kg\ H_2O/kg\ O_2\}$$
$$f_{32} = 0.333 \quad \{kg\ CH_4/kg\ O_2\}$$
$$f_{44} = 0.583 \quad \{kg\ CO/kg\ O_2\}.$$

Combustion of CH_x

$$R_{14} \leq G_7/f_{35} \quad \{kg\ O_2/m^2 \cdot s\}$$

where:

$$H_{14} = 1.08 \times 10^{7} \quad \{J/kg\ O_2\}$$
$$f_{33} = 0. \quad \{kg\ CO_2/kg\ O_2\}$$
$$f_{34} = 0.608 \quad \{kg\ H_2O/kg\ O_2\}$$
$$f_{35} = 0.414 \quad \{kg\ CH_x/kg\ O_2\}$$
$$f_{45} = 0.806 \quad \{kg\ CO/kg\ O_2\}.$$

Combustion of CO

$$R_{15} \leq G_4/f_{37} \quad \{kg\ O_2/m^2 \cdot s\}$$

where:

$$H_{15} = 1.77 \times 10^{7} \quad \{J/kg\ O_2\}$$
$$f_{36} = 2.751 \quad \{kg\ CO_2/kg\ O_2\}$$
$$f_{37} = 1.751 \quad \{kg\ CO/kg\ O_2\}.$$

Combustion of Oil

Two options are permitted for oil combustion. In both options, the heat of reaction and stoichiometry factors are

$$H_{16} = 9.88 \times 10^6 \quad \{J/kg\ O_2\}$$
$$f_{38} = 0. \quad \{kg\ CO_2/kg\ O_2\}$$
$$f_{39} = 0.988 \quad \{kg\ CO/kg\ O_2\}$$
$$f_{40} = 0.507 \quad \{kg\ H_2O/kg\ O_2\}$$
$$f_{41} = 0.495 \quad \{kg\ oil/kg\ O_2\}$$
$$f_{42} = 0. \quad \{kg\ CH_4/kg\ O_2\}$$
$$f_{43} = 0. \quad \{kg\ CH_x/kg\ O_2\}.$$

Option 1 for oil combustion is similar to the previous gas combustion rate equations; i.e.,

$$R_{16} \leq G_9/f_{41} \quad \{kg\ O_2/m^2 \cdot s\}.$$

This equation appears to be a reasonable one to use. Unfortunately, it gives erratic results unless a very fine axial grid is used. The erratic results are due to the periodic nature of oil generation as a function of time when the usual axial grid is used. For most applications it is prohibitive to use a fine enough grid interval to obtain accurate results with option 1. A fine-mesh, moving grid in the region of kerogen decomposition is being implemented to hopefully alleviate this problem. Although the current model does have the capability for using such a moving grid, it has not been exhaustively tested and therefore is not yet recommended for general use.

Option 2 for oil burn is the recommended one. The rate equation is

$$R_{16} \leq G_2 - \sum_{j=1}^{N_p} \alpha_j (R_8)_j \Delta z \quad \{kg\ O_2/m^2 \cdot s\}.$$

The summation term in this equation is the net consumption of oxygen by reaction with the organic carbon residue in the N_p particle size classes in the interval Δz. In this option, not only the released oil vapor (G_9) can be burned, but also the potential oil vapor from yet to be pyrolyzed kerogen in

the interval Δz is allowed to burn. This option avoids the erratic results found with option 1 and appears to simulate the actual oil combustion quite accurately. During the initial ignition phase of the retort, option 1 is still used until the specified ignition criteria have been satisfied.

Constraints on Gas Combustion Reactions

Several constraints are imposed on the solution of the rate equations for gas and oil combustion:

(1) No reaction is permitted unless the gas temperature exceeds a specified threshold temperature (normally 400°C).

(2) The total oxygen consumption by carbon, gas, and oil combustion is limited by the oxygen flux; i.e.,

$$\sum_{j=1}^{N_p} \alpha_j (R_8)_j \Delta z + \sum_{i=12}^{16} R_i \leq G_2 \quad .$$

(3) The combustion reactions in the bulk-gas stream are calculated in the following sequence after the carbon combustion reaction. First, oil combustion is calculated. Then there are two options for oxidizing the other four gas species. In option 1, the gases are assumed to preferentially burn in the sequence H_2, CH_x, CH_4, and CO (i.e., R_{12}, R_{14}, R_{13}, and R_{15}). In option 2, the gases are assumed to burn simultaneously, each in proportion to its maximum rate R_i. Option 1 is recommended.

CRACKING OF OIL VAPOR IN BULK-GAS STREAM

In MIS combustion retorting, the oil emerging from blocks of oil shale enters the bulk-gas stream that may be 200°C hotter than the block surface. Because this gas stream may also contain O_2, a loss in oil yield may take place by both combustion and cracking. The rate of cracking is

$$R_{17} = G_9 \left[1 - \exp(-k_{17}\tau)\right] \{\text{kg oil/m}^2 \cdot \text{s}\} \ ,$$

where:

$$\tau = \varepsilon\left(\frac{P_0}{RT}\right)\Delta z \Big/ \sum_{i=1}^{8}\left(\frac{G_i}{M_i}\right) \quad \{s\}$$

$$k_{17} = 4.8 \times 10^8 \exp(-19340/T) \quad \{s^{-1}\}$$

$$f_{46} = 0.03 \quad \{\text{kg CO/kg oil}\}$$

$$f_{47} = 0.02 \quad \{\text{kg } H_2\text{/kg oil}\}$$

$$f_{48} = 0.11 \quad \{\text{kg } CH_4\text{/kg oil}\}$$

$$f_{49} = 0.53 \quad \{\text{kg } CH_x\text{/kg oil}\}$$

$$1-f_{46}-f_{47}-f_{48}-f_{49} = 0.31 \quad \{\text{kg C/kg oil}\} .$$

The rate coefficient (k_{17}) and stoichiometry factors were measured by Burnham.[43] Comparisons of model calculations, particularly offgas composition, with experimental retort data do not fully support the use of these values. Therefore, it is recommended that this reaction be disabled until improved kinetics and stoichiometry for both combustion and cracking of oil vapor are available.

MASS BALANCE EQUATIONS

The mass balance equations can now be directly written in terms of the reaction rates in the previous section. These equations are defined at each axial grid point. The equations for the shale phase are defined for each of the N_p particle sizes. If desired, the equations for U_1, U_2, and U_3 can also be defined as a function of radial location within the shale particle by zoning the particle into a specified number of equivolume, concentric spherical shells.

SHALE PHASE

$$\frac{\partial U_i}{\partial t} = -R_i, \; i = 1, \; 2, \; 3, \text{ and } 4$$

$$\frac{\partial U_5}{\partial t} = f_2 R_1 - R_5$$

$$\frac{\partial U_6}{\partial t} = f_1 R_1 - f_{13} R_6 - f_{17} R_7 - f_{20} R_8 + f_{21} R_9 + (1 - f_{46} - f_{47} - f_{48} - f_{49}) R_{17} / [\Delta z (1 - \varepsilon)]$$

FLUID PHASE

$$\frac{\partial G_1}{\partial z} = 0$$

$$\frac{\partial G_2}{\partial z} = - \sum_{i=12}^{16} R_i / \Delta z - \sum_{j=1}^{N_p} \alpha_j (R_8)_j$$

$$\frac{\partial G_3}{\partial z} = (f_{25} R_{11} + f_{30} R_{13} + f_{33} R_{14} + f_{36} R_{15} + f_{38} R_{16}) / \Delta z + \sum_{j=1}^{N_p} \alpha_j (f_5 R_1 + R_2 + R_3 - R_6 + f_{14} R_7 + f_{18} R_8)_j$$

$$\frac{\partial G_4}{\partial z} = (-f_{27} R_{11} + f_{44} R_{13} + f_{45} R_{14} - f_{37} R_{15} + f_{39} R_{16} + f_{46} R_{17}) / \Delta z + \sum_{j=1}^{N_p} \alpha_j (f_4 R_1 + f_{12} R_6 + f_{15} R_7 + f_{19} R_8)_j$$

$$\frac{\partial G_5}{\partial z} = (f_{26}R_{11} - f_{29}R_{12} + f_{47}R_{17})/\Delta z + \sum_{j=1}^{N_p} \alpha_j (f_6 R_1 + R_5 + f_{16}R_7 + f_{22}R_9)_j$$

$$\frac{\partial G_6}{\partial z} = (-f_{32}R_{13} + f_{42}R_{16} + f_{48}R_{17})/\Delta z + \sum_{j=1}^{N_p} \alpha_j (f_7 R_1 + f_{23}R_9)_j$$

$$\frac{\partial G_7}{\partial z} = (-f_{35}R_{14} + f_{43}R_{16} + f_{49}R_{17})/\Delta z + \sum_{j=1}^{N_p} \alpha_j (f_8 R_1)_j$$

$$\frac{\partial G_8}{\partial z} = (-R_{10} - R_{11} + f_{28}R_{12} + f_{31}R_{13} + f_{34}R_{14} + f_{40}R_{16})/\Delta z + \sum_{j=1}^{N_p} \alpha_j (f_9 R_1 + R_4 - R_7 + f_{24}R_9)_j$$

$$\frac{\partial G_9}{\partial z} = -(f_{41}R_{16} + R_{17})/\Delta z + \sum_{j=1}^{N_p} \alpha_j (f_3 R_1 - R_9)_j$$

$$\frac{\partial G_{10}}{\partial z} = R_{10}/\Delta z$$

ENERGY BALANCE EQUATIONS

As with the mass balance equations, zoning of the shale particles may be used in order to obtain the shale temperature (T_j) as a function of radial location within the shale particles. The temperature of the surface zone is designated T_{1j}. The physical properties used in the following equations are given in Appendix A.

The energy balance equation for the solid phase (particle size class j) is

$$\rho_j C_j \frac{\partial T_j}{\partial t} = \frac{1}{r^2} \frac{\partial}{\partial r}\left(r^2 \lambda_j \frac{\partial T_j}{\partial r}\right) + Q_j \quad ,$$

where the boundary conditions are

$$\lambda_j \frac{\partial T_j}{\partial r} = h_j (T_g - T_{lj}), \text{ at } r = r_j$$

and

$$\frac{\partial T_j}{\partial r} = 0, \text{ at } r = 0.$$

The energy balance equation for the fluid phase is

$$\frac{\partial}{\partial z}\left(k_e \frac{\partial T_g}{\partial z}\right) - C_g G \frac{\partial T_g}{\partial z} - \sum_{j=1}^{N_p} \left[\frac{3\alpha_j h_j}{r_j} (T_g - T_{lj})\right] - \frac{4\lambda_W}{D_R D_W} (T_g - T_W) + Q_g = 0,$$

where the boundary conditions are

$$T_g = F(t) + \frac{k_e}{C_g G} \frac{\partial T_g}{\partial z} \quad , \quad \text{at } z = 0$$

and

$$\frac{\partial T_g}{\partial z} = 0, \quad \text{at } z = z_{max} \quad .$$

We have used the quasi-steady-state approximation for the gas energy equation. This approximation should be valid, because the small mass of the gas (compared with that of the solid) causes the gas properties to be primarily determined by interaction with the solid phase rather than by the past history of the gas phase.

The heats of reaction for the above energy balance equations are

$$Q_g = \sum_{i=11}^{17} H_i R_i / \Delta z$$

and

$$Q_j = \left[\sum_{i=1}^{9} H_i R_i\right]_j + \frac{\delta H_{10} R_{10}}{(1 - \varepsilon)\Delta z} \quad .$$

Note that the heat for water condensation or vaporization is applied only to the surface zone of each particle; i.e., $\delta = N_j$ for the surface zone and $\delta = 0$ for other interior zones.

SOLUTION PROCEDURE

The governing equations are solved by means of a semi-implicit, finite-difference method (see Appendix B). Modification of the numerical method to enable simulation of moving-bed retorting is discussed in Appendix C. The computer program is written in LRLTRAN (an LLNL extended version of FORTRAN) for use on a CDC-7600 or CRAY computer. A listing of the computer program can be obtained from the author.

APPLICATION OF MODEL

Throughout the course of the development, the model has been constantly applied to laboratory pilot retorting conditions as well as in field conditions (Braun and Chin,[44] Braun,[45] Carley and Braun,[46] and Lewis and Braun[47]). It has been a good frame of reference in our experimental program in the sense of (1) helping to identify sensitive variables that may require further laboratory measurements and (2) helping to plan expensive laboratory retort experiments so that they will yield the most significant information.

The model has been used to predict the results of *in situ* retorting under a variety of conditions, thereby helping to determine operating conditions and control schemes for commercial-scale retorting.

The model has been tested by the comparison of calculated results with data from laboratory retort experiments performed with controlled heat loss at the wall. Reasonable agreement is generally found for retorting rate, oil yield, offgas composition, and temperature profile.[45] An exception to this is that for rich shale (>30 gal/ton) the calculated maximum retort temperature is too high, typically by 100 to 200°C. The model is being evaluated further in order to better determine its accuracy and to help to establish which of its aspects need improvement. Some specific problem areas have already been indicated in this report.

ACKNOWLEDGMENTS

Technical discussions with members of the LLNL Oil Shale Group contributed to the development and application of this model. In particular, contributions of A. E. Lewis, A. J. Rothman, R. G. Mallon, J. F. Carley, J. H. Raley, J. H. Campbell, A. K. Burnham, and H. Y. Sohn are gratefully acknowledged. R. C. Y. Chin provided valuable assistance in developing the numerical procedures used in solving the model equations and D. R. McKenzie in carrying out the computer calculations.

APPENDIX A

PHYSICAL PROPERTIES

FLUID HEAT CAPACITIES (J/kg·K)

The heat capacities of the gas species at constant pressure are approximated by quadratic equations over the temperature interval from 300 to 1500 K (Hougen et al.[48]). The heat capacities for N_2, O_2, CO_2, CO, H_2, CH_4, CH_x, H_2O, and oil vapor are, respectively,

$$C_{g1} = 964.86 + 0.20756\ T - 0.0000103\ T^2$$
$$C_{g2} = 799.8 + 0.41409\ T - 0.0001314\ T^2$$
$$C_{g3} = 602.78 + 0.96422\ T - 0.00032474\ T^2$$
$$C_{g4} = 948.87 + 0.27062\ T - 0.000040\ T^2$$
$$C_{g5} = 14415.7 - 0.40678\ T + 0.00098727\ T^2$$
$$C_{g6} = 837.85 + 4.8142\ T - 0.0011715\ T^2$$
$$C_{g7} = 323.09 + 5.29296\ T - 0.0015264\ T^2$$
$$C_{g8} = 1658.72 + 0.61365\ T + 0.0000107\ T^2$$
$$C_{g9} = -181.74 + 5.90538\ T - 0.0020741\ T^2$$

The heat capacity of liquid water is taken to be constant: $C_{g10} = 4184$. The product $C_g G$ for use in the fluid energy equation is then

$$C_g G = \sum_{i=1}^{10} C_{gi} G_i \quad .$$

SHALE HEAT CAPACITY (J/kg·K)

The heat capacity of raw and spent shale (Carley[19]) is

$$C = (906.9 + 506\ W_K)(1 - f_K) + 827.4\ f_K$$
$$+ [(0.6184 + 5.56\ W_K)(1 - f_K) + 0.922\ f_K](T - 298),$$

where:

W_K = weight fraction kerogen in raw shale

f_K = fraction of kerogen pyrolyzed.

SHALE DENSITY (kg/m^{3}shale)

$$\rho = \rho^o + \sum_{i=1}^{6} U_i \quad ,$$

where ρ^o is the contribution of all nonvolatilizable components to the bulk shale density.

SHALE THERMAL CONDUCTIVITY (J/m·K·s)

The thermal conductivity of raw, spent, and burned shale has been measured by Tihen et al.[49] as a function of shale grade, both parallel and perpendicular to the bedding planes. Their data is applied as follows. When kerogen is present, interpolation is made between raw and spent shale on the basis of the fraction of kerogen remaining:

$$\lambda = \lambda_R \left(\frac{U_1}{U_1^o}\right) + \lambda_S \left(1 - \frac{U_1}{U_1^o}\right) .$$

When kerogen is not present, interpolation is made between spent and burned shale on the basis of the fraction of residual organic carbon remaining:

$$\lambda = \lambda_S \left(\frac{U_6}{U_6^o}\right) + \lambda_B \left(1 - \frac{U_6}{U_6^o}\right) \quad ,$$

where λ_R, λ_S, and λ_B are the thermal conductivities for raw, spent, and burned shale, respectively, averaged for the measured values parallel and perpendicular to the bedding planes for the shale grade of interest. The minor temperature dependence of the thermal conductivity is ignored.

EFFECTIVE AXIAL THERMAL CONDUCTIVITY (J/m·K·s)

Hlavecek and Votruba[50] recommend that the effective axial thermal conductivity be used with the gas phase transport equation. Yagi et al.[51,52] give correlations for estimating the effective axial thermal dispersion coefficient. An approximation of their correlation is

$$k_e = k_{e1}(1 - \varepsilon) + k_{e2}\varepsilon D_p T_g^3 + k_{e3} C_g G D_p ,$$

where $k_{e1} = 0.56$, $k_{e2} = 2.27 \times 10^{-7}$, and $k_{e3} = 0.7$. It is not clear how the particle size distribution should be averaged for the second and third terms. Comparison of thermal profiles from the LLNL small retort with model calculations using either the surface-to-volume mean particle diameter or the mass average particle diameter indicates too great a calculated thermal dispersion. The best results are obtained simply with k_{e2} and k_{e3} both zero. Therefore, current model calculations use only the first term for k_e, until the effects of the other terms can be better understood.

GAS-SOLID HEAT AND MASS TRANSFER COEFFICIENT

Carley[53] has experimentally shown that gas-solid mass transfer coefficients depend on the individual particle sizes (r_j) of a packed bed rather than on the average particle size; i.e.,

$$\ell n \left[\frac{k_d \rho_g (N_{Sc})^{2/3}}{G} \right] = 0.2952 - 0.4675 \ \ell n \ N_{Re} + 0.01309 \ (\ell n \ N_{Re})^2 ,$$

where the modified Reynolds number is

$$N_{Re} = \frac{2 r_j G}{1.5 \ \mu (1 - \varepsilon)} .$$

By analogy, the gas-solid heat transfer coefficient can also be expressed as a function of the individual particle radius:

$$\ell n \left[\frac{h (N_{Pr})^{2/3}}{C_g G} \right] = 0.2952 - 0.4675 \ \ell n \ N_{Re} + 0.01309 \ (\ell n \ N_{Re})^2 .$$

In evaluating k_d and h from these equations, the following values are used:

$$N_{Sc} = N_{Pr} = 0.69$$

and

$$\mu = 3.5 \times 10^{-7} T^{0.68} \quad \{kg/m \cdot s\} .$$

VAPOR PRESSURE OF WATER (Pa)

The vapor pressure of water is closely approximated by the equation,

$$\hat{P}_{H_2O} = 1.1833 \times 10^{10} \exp[-3818.15/(T - 45.92)] .$$

EFFECTIVE DIFFUSIVITIES OF O_2 AND H_2O (m^2/s)

The effective diffusivity of O_2 in the direction of the bedding planes was measured by Mallon and Braun[24] in cylindrical blocks of spent shale. The measured effective diffusivity could be approximated by

$$D_{e,O_2} = D_{O_2} \varepsilon_k^2 ,$$

where the molecular diffusivity of O_2, taken from Wilke and Lee[54] for the CO_2-air system, is

$$D_{O_2} = 1.48 \times 10^{-9} T^{1.65}$$

and the shale porosity produced by complete removal of kerogen is

$$\varepsilon_k = U_1^o/1060 .$$

The block experiments also qualitatively indicated that the diffusivity perpendicular to the bedding planes is about one half that for parallel

transport. Thus, the correct value for a piece of oil shale is about 80% of the value obtained for parallel transport; i.e.,

$$D_{e,O_2} = 1.04 \times 10^{-15} \left(U_1^o\right)^2 T^{1.65} \quad .$$

The effective diffusivity of H_2O in spent shale was not measured, but by analogy to O_2 is

$$D_{e,H_2O} = D_{H_2O} \varepsilon_k^2$$

where the molecular diffusivity of H_2O, estimated from equations in Hirschfelder et al.[55] for the H_2O-CO_2 system, is

$$D_{H_2O} = 1.06 \times 10^{-9} T^{1.73} \quad .$$

Again applying the 80% geometric factor, the effective diffusivity should be

$$D_{e,H_2O} = 7.4 \times 10^{-16} \left(U_1^o\right)^2 T^{1.73} \quad .$$

APPENDIX B

NUMERICAL METHODS

In developing an efficient computational method, the time scale differences must be carefully considered for the chemical and physical phenomena involved. A scheme that does not take advantage of these disparate scales must necessarily be inefficient. Moreover, the question of accuracy is totally subjective. At times, it is expedient to sacrifice "some" accuracy to achieve efficiency. Several numerical methods were explored. The method discussed here was selected because of its simplicity and efficiency.

Examination of the governing equations shows that the gas-solid heat transfer process constitutes one of the characteristic time scales of interest. At low temperatures, this process is the dominant phenomenon. As temperature increases, chemistry comes into play as various reaction rates become comparable to the heat transfer rate and then surpass it at higher temperatures. This wide range in reaction rates is typical of a stiff system of equations (Gear,[56] Lapidus and Seinfeld[57]). An obvious implication is that a fully implicit, stiffly stable algorithm with dynamic step-size control is required to integrate the equations if strict accuracy is to be maintained. However, it is believed that the cost of developing and implementing a dynamic scheme to control the space and time steps outweighs the benefits for this application. Moreover, since the kinetics of some of the gaseous reactions are not known, a fully implicit formulation is not possible. Therefore, a fixed-step-size, semi-implicit method is pursued.

The numerical procedure developed to solve the model equations parallels the procedure described previously by Braun and Chin.[12] The present model, however, recognizes temperature and compositional gradients within a shale particle, whereas the earlier model assumed that these properties were uniform throughout the shale particle. Handling these gradients is accomplished by using zoned particles, with N_j zones in particle size class j. Only intraparticle gradients in temperature, kerogen, $MgCO_3$, and $CaCO_3$ are permitted.

Let $\underline{U}$ be the shale composition vector; i.e.,

$$\underline{U} = \left[\{U_1, U_2, U_3\}_{k=1}^{N_j}, U_4, U_5, U_6\right]_{j=1}^{N_p} ,$$

and $\underline{G}$ be the fluid composition vector; i.e.,

$$\underline{G} = \{G_1, G_2, \ldots, G_{10}\} .$$

Thus, the mass balance equations can be written:

$$\frac{\partial \underline{U}}{\partial t} = -\underline{F}(\underline{U}, \underline{G}, T_{kj}, T_g) \tag{B1}$$

and

$$\frac{\partial \underline{G}}{\partial z} = \underline{V}(\underline{U}, \underline{G}, T_{kj}, T_g) \tag{B2}$$

for $1 \le j \le N_p$ and $1 \le k \le N_j$.

Suppose we have the solution at $t = t^{n-1}$. To advance one time step Δt to $t = t^n$, we use a first-order Euler formula to integrate Eq. (B1); i.e.,

$$\underline{U}_i^n = \underline{U}_i^{n-1} - \Delta t \, \underline{F}_i^{n-1}, \quad i = 1, \ldots, N_z$$

where:

$$\underline{F}_i^{n-1} \equiv \underline{F}\left(\underline{U}_i^{n-1}, \underline{G}_i^*, T_{kji}^{n-1}, T_{g_i}^{n-1}\right) ,$$

and

$$\underline{G}_i^* = \underline{G}_{i-1}^n + \frac{1}{2}\Delta z \, \underline{V}\left(\underline{U}_{i-1}^n, \underline{G}_{i-1}^n, T_{kji}^{n-1}, T_{g_{i-1}}^{n-1}\right) .$$

To ensure that $\underline{U}_i^n \geq 0$ and $\underline{G}_i^* \geq 0$, we apply the following cutoff for all i:

$$\text{if } \Delta t\, \underline{F}_i^{n-1} \geq \underline{U}_i^{n-1} ,$$

$$\text{then } \underline{U}_i^n \equiv 0.$$

Similarly

$$\text{if } \Delta \underline{G}_{i-1}^n = \left(\underline{G}_i^* - \underline{G}_{i-1}^n\right) \geq \underline{G}_{i-1}^n ,$$

$$\text{then } \underline{G}_i^* \equiv 0.$$

The next step in the numerical procedure is to advance $\underline{G}$. To do so, we use a trapezoidal rule (Henrici[58]) with the temperature variables evaluated at the previous time step; i.e.,

$$\underline{G}_i^n - \underline{G}_{i-1}^n = \frac{1}{2}\Delta z \left(\underline{V}_i^n + \underline{V}_{i-1}^n\right) ,$$

where

$$\underline{V}_i^n \equiv \underline{V}\left(\underline{U}_i^n,\ \underline{G}_i^n,\ T_{kji}^{n-1},\ T_{g_i}^{n-1}\right) .$$

Similar cutoffs are applied here. The remaining step is the solution of the temperature equations. Note that by this time $\left\{\underline{G}_i^n\right\}$ and $\left\{\underline{U}_i^n\right\}$ have been computed and, therefore, terms dependent on these values are known.

To formulate the solution of the temperature equations, we begin by writing the gas energy equation as a first-order system; i.e.,

$$k_e \frac{\partial T_g}{\partial z} = P \tag{B3}$$

and

$$\frac{\partial P}{\partial z} = C_g G \frac{\partial T_g}{\partial z} + \sum_{j=1}^{N_p} \left[\frac{3\alpha_j h_j}{r_j}\left(T_g - T_{lj}\right)\right] + \frac{4\lambda_W}{D_R D_W}\left(T_g - T_W\right) - Q_g \quad . \tag{B4}$$

To generate a discrete set of equations, we use the trapezoidal rule (Keller[59]). Equations (B3) and (B4) then become, respectively,

$$\frac{k_e}{\Delta z}\left(T^n_{g_i} - T^n_{g_{i-1}}\right) = \frac{1}{2}\left(P^n_i + P^n_{i-1}\right) \tag{B5}$$

and

$$P^n_i - P^n_{i-1} = \frac{1}{2}\left[(C_g G)^n_i + (C_g G)^n_{i-1}\right]\left(T^n_{g_i} - T^n_{g_{i-1}}\right)$$

$$+ \frac{3}{2}\Delta z \sum_{j=1}^{N_p} \frac{\alpha_j}{r_j}\left[h^n_{ji}\left(T^n_{g_i} - T^n_{lji}\right) + h^n_{j,i-1}\left(T^n_{g_{i-1}} - T^n_{lj,i-1}\right)\right]$$

$$+ \frac{2\lambda_W}{D_R D_W}\Delta z\left(T^n_{g_i} + T^n_{g_{i-1}} - 2T_W\right) - \frac{1}{2}\Delta z\left(Q^n_{g_i} + Q^n_{g_{i-1}}\right), \tag{B6}$$

for $j = 1, \ldots, N_p$ and $i = 2, \ldots, N_z$.

Discretization of the shale energy equations is based on zoning of each shale particle into equivolume, spherically concentric shells. For the surface zone ($k = 1$),

$$\frac{1}{2\Delta t}\left[\left(\rho_{kj}C_{kj}\right)^n_i + \left(\rho_{kj}C_{kj}\right)^{n-1}_i\right]\left(T^n_{kji} - T^{n-1}_{kji}\right)$$

$$- \frac{3N_j}{2r_j}\left[h^n_{ji}\left(T^n_{g_i} - T^n_{kji}\right) + h^{n-1}_{ji}\left(T^{n-1}_{g_i} - T^{n-1}_{kji}\right)\right]$$

$$+ \left(\frac{a^2_{k+1}}{a_k - a_{k+2}}\right)\frac{3N_j}{r_j^2}\left[\lambda^n_{ji}\left(T^n_{kji} - T^n_{k+1,ji}\right) + \lambda^{n-1}_{ji}\left(T^{n-1}_{kji} - T^{n-1}_{k+1,ji}\right)\right]$$

$$= \frac{1}{2}\left(Q^n_{kji} + Q^{n-1}_{kji}\right). \tag{B7}$$

For the inner zones ($1 < k < N_j$),

$$\frac{1}{2\Delta t}\left[\left(\rho_{kj}C_{kj}\right)_i^n + \left(\rho_{kj}C_{kj}\right)_i^{n-1}\right]\left(T_{kji}^n - T_{kji}^{n-1}\right)$$

$$-\left(\frac{a_k^2}{a_{k-1} - a_{k+1}}\right)\frac{3N_j}{r_j^2}\left[\lambda_{ji}^n\left(T_{k-1,ji}^n - T_{kji}^n\right) + \lambda_{ji}^{n-1}\left(T_{k-1,ji}^{n-1} - T_{kji}^{n-1}\right)\right]$$

$$+\left(\frac{a_{k+1}^2}{a_k - a_{k+2}}\right)\frac{3N_j}{r_j^2}\left[\lambda_{ji}^n\left(T_{kji}^n - T_{k+1,ji}^n\right) + \lambda_{ji}^{n-1}\left(T_{kji}^{n-1} - T_{k+1,ji}^{n-1}\right)\right]$$

$$= \frac{1}{2}\left(Q_{kji}^n + Q_{kji}^{n-1}\right). \qquad \text{(B8)}$$

For the central zone ($k = N_j$),

$$\frac{1}{2\Delta t}\left[\left(\rho_{kj}C_{kj}\right)_i^n + \left(\rho_{kj}C_{kj}\right)_i^{n-1}\right]\left(T_{kji}^n - T_{kji}^{n-1}\right)$$

$$-\left(\frac{a_k^2}{a_{k-1} - a_{k+1}}\right)\frac{3N_j}{r_j^2}\left[\lambda_{ji}^n\left(T_{k-1,ji}^n - T_{kji}^n\right) + \lambda_{ji}^{n-1}\left(T_{k-1,ji}^{n-1} - T_{kji}^{n-1}\right)\right]$$

$$= \frac{1}{2}\left(Q_{kji}^n + Q_{kji}^{n-1}\right). \qquad \text{(B9)}$$

In the preceding equations, $a_1 = 1$ and equivolume zoning for spherical shale particles is obtained by using

$$a_k = \left(a_{k-1}^3 - \frac{1}{N_j}\right)^{1/3}.$$

LU decomposition of Eqs. (B7), (B8), and (B9) gives the new temperature of the surface zone of each particle $\left(T_{1ji}^n\right)$ as an implicit function of the new gas temperature $\left(T_{g_i}^n\right)$. These functions are substituted into Eq. (B6). Then Eqs. (B5) and (B6) are solved for $\left(T_{g_i}^n\right)$ using the discrete invariant imbedding algorithm previously used[12] and described more completely by Chin and Braun.[60] Once $\left(T_{g_i}^n\right)$ is known, the new shale temperatures $\left(T_{kji}^n\right)$ are readily obtained from Eqs. (B7), (B8), and (B9).

APPENDIX C

EXTENSION TO MOVING-BED RETORT

After development of the present model to simulate batch processing of oil shale was well underway, the need for a model to simulate continuous processing of oil shale arose. Therefore, the existing model was modified to calculate the retorting of shale moving through a retort, as required for a continuous process in surface equipment. This modification was accomplished most readily by a minor change in the existing numerical procedure described in Appendix B. For each time interval in the calculation, after solution of the energy equations, we calculate the incremental change in axial location corresponding to the specified linear velocity of the shale particles during that time interval. Then all of the stored values for shale composition and other properties are shifted the required number of axial grid points. Any fractional increment of axial grid spacing is accumulated until the next time step. If desired, the properties of the inlet shale (temperature, composition, particle size, bed porosity, and linear velocity) as well as the properties of the inlet gas (temperature, composition, and flow rate) can be changed as a function of time.

An additional requirement for simulating certain surface retorting processes is that injection of gas or liquid water be allowed at locations other than $z = 0$. This requirement was incorporated into the numerical procedures as follows. If the additional gas is to be introduced at axial grid point i (where $1 < i < N_z$), then $\underline{G}_i^n$ is incremented by the new input values before solution of Eqs. (B1) and (B2). The enthalpy change of the injected gas from the injection temperature to the bulk-gas temperature is included in Q_g. The effects of any heat exchange process that may be used to cool the air injection lines is also included in Q_g.

REFERENCES

1. A. E. Lewis and A. J. Rothman, *Rubble In Situ Extraction (RISE): A Proposed Program for Recovery of Oil from Oil Shale*, Lawrence Livermore National Laboratory, Report UCRL-51768 (1975).
2. A. J. Rothman, *Recent Experimental Developments in Retorting Oil Shale at the Lawrence Livermore Laboratory*, Lawrence Livermore National Laboratory, Report UCRL-83569 (1979).
3. E. F. Kondis, D. W. Lewis, M. T. Siuta, and P. W. Snyder, "Development and Utilization of a Model for Evaluating Aboveground and In Situ Retorting of Oil Shale," *Proc. of 79th National Meeting of AIChE*, Houston TX (1975).
4. W. F. Johnson, D. K. Walton, H. H. Keller and E. J. Couch, "In Situ Retorting of Oil Shale Rubble: A Model of Heat Transfer and Product Formation in Oil Shale Particles," *Colorado School of Mines Quart.*, 70, 237 (1975).
5. H. E. McCarthy and C. Y. Cha, "Oxy Modified In Situ Process Development and Up-date," *Colorado School of Mines Quart.*, 71, 85 (1976).
6. D. W. Fausett, "A Mathematical Model of an Oil Shale Retort," *Colorado School of Mines Quart.*, 70, 272 (1975).
7. H. E. Nuttall, "Mathematical Modeling and Experimental Investigation of Oil Shale Retorting," *Proc. of 51st Annual Meeting SPE-AIME*, New Orleans (1976).
8. L. Dockter and H. G. Harris, "A Mathematical Model of Forward Combustion Retorting of Oil Shale," Laramie Energy Technology Center, Report LETC/TPR-78/1 (1978).
9. J. H. George and H. G. Harris, "Mathematical Modeling of In Situ Oil Shale Retorting," *SIAM Numerical Analysis J.*, 14, 137 (1977).
10. J. H. George and H. G. Harris, *Mathematical Modeling of In Situ Oil Shale Retorting--Final Report*, Department of Mathematics, University of Wyoming, Laramine, WY, Report FE-2234-T1 (1978).
11. B. R. Bowman, *A Computational Model for Oil Shale Retorting*, Lawrence Livermore National Laboratory, Report UCRL-51780 (1976).
12. R. L. Braun and R. C. Y. Chin, *Progress Report on Computer Model for In Situ Oil Shale Retorting*, Lawrence Livermore National Laboratory, Report UCRL-52292 (1977).

13. A. B. Hubbard and W. E. Robinson, *A Thermal Decomposition Study of Colorado Oil Shale,* U.S. Bureau of Mines, Washington, D.C., Report 4744 (1950).

14. V. D. Allred, "Kinetics of Oil Shale Pyrolysis," *Chem. Eng. Prog.* 62, 55 (1966).

15. J. J. Cummins and W. E. Robinson, *Controlled Low-Temperature Pyrolysis of Benzene-Extracted Green River Oil Shale,* U.S. Bureau of Mines, Washington, D.C., Report 7620 (1972).

16. R. L. Braun and A. J. Rothman, "Oil Shale Pyrolysis: Kinetics and Mechanism of Oil Production," *FUEL,* 54, 129 (1975).

17. J. H. Campbell, G. J. Koskinas, and N. Stout, *The Kinetics of Decomposition of Colorado Oil Shale: I. Oil Generation,* Lawrence Livermore National Laboratory, Report UCRL-52089 (1976).

18. J. W. Smith, *Ultimate Composition of Organic Material in Green River Oil Shale,* U.S. Bureau of Mines, Washington, D.C., Report of Investigations 5725 (1961).

19. J. F. Carley, "Heat of Kerogen Decomposition and Improved Enthalpy-Temperature Relationships for Raw and Spent Colorado Oil Shales," Lawrence Livermore National Laboratory, Oil Shale Project Memo, UOPKK 75-28 (1975).

20. J. R. Raley, LLNL, private communication (1977).

21. J. W. Smith, *Analytical Method for Study of Thermal Degradation of Oil Shale,* U.S. Bureau of Mines, Washington, D.C., Report of Investigations 5932 (1962).

22. J. H. Campbell, G. Gallegos, and M. Gregg, "Gas Evolution During Oil Shale Pyrolysis. 2. Kinetic and Stoichiometric Analysis," *FUEL,* 59, 727 (1980).

23. J. H. Campbell, *The Kinetics of Decomposition of Colorado Oil Shale: II. Carbonate Minerals,* Lawrence Livermore National Laboratory, Report UCRL-52089 Part 2 (1978).

24. R. G. Mallon and R. L. Braun, "Reactivity of Oil Shale Carbonaceous Residue with Oxygen and Carbon Dioxide," *Colorado School of Mines Quart.,* 71, 309 (1976).

25. A. K. Burnham, *Studies of Oil Shale Reaction Chemistry at LLL,* Lawrence Livermore National Laboratory, Report UCRL-83568 (1979).

26. R. L. Braun, R. G. Mallon, and H. Y. Sohn, *Analysis of Multiple Gas-Solid Reactions During the Gasification of Char in Oil Shale Blocks,* Lawrence Livermore National Laboratory, Report UCRL-85279 (1981).

27. J. H. Campbell, G. J. Koskinas, T. Coburn, and N. Stout, "Dynamics of Oil Evolution During Retorting of Oil Shale Blocks and Powders," *Proc. 10th Oil Shale Symposium,* Colorado School of Mines, Golden, CO (1977).

28. H. Y. Sohn, "The Law of Additive Reaction Times in Fluid-Solid Reactions," *Met. Trans. B,* 9B, 89 (1978).

29. H. Y. Sohn and R. L. Braun, "Simultaneous Fluid-Solid Reactions in Porous Solids: Reactions Between One Solid and Two Fluid Reactants," *Chem. Eng. Sci.,* 35, 1625 (1980).

30. A. K. Burnham, "Reaction Kinetics Between CO_2 and Oil-Shale Residual Carbon. 1. Effect of Heating Rate on Reactivity," *FUEL,* 58, 285 (1979).

31. A. K. Burnham, "Reaction Kinetics Between CO_2 and Oil-Shale Residual Carbon. 2. Partial-Pressure and Catalytic-Mineral Effects," *FUEL,* 58, 713 (1979).

32. W. J. Thomson, M. A. Gerber, M. A. Hatter and D. G. Oakes, "Kinetics of Oil Shale Char Gasification," *Proc. A.C.S. Symp. on Oil Shale, Tar Sands and Related Materials,* San Francisco, CA (1980).

33. M. L. Gregg, J. H. Campbell, and J. R. Taylor, *Laboratory and Modeling Investigation of Oil-Shale Block Retorting to 900°C,* Lawrence Livermore National Laboratory, Report UCRL-83265 (1979).

34. S. Ergun, "Kinetics of the Reaction of Carbon Dioxide with Carbon," *J. Phys. Chem.,* 60, 480 (1956).

35. R. W. Taylor and D. W. Bowan, *Rate of Reaction of Steam and Carbon Dioxide with Chars Produced from Subbituminous Coals,* Lawrence Livermore National Laboratory, Report UCRL-52002 (1976).

36. H. Y. Sohn and H. J. Sohn, "The Effect of Bulk Flow Due to Volume Change in the Gas Phase on Gas-Solid Reactions: Initially Nonporous Solids," *Ind. Eng. Chem. Process Des. Dev.,* 19, 237 (1980)

37. A. K. Burnham, "Reaction Kinetics Between Steam and Oil-Shale Residual Carbon," *FUEL,* 58, 719 (1979).

38. A. K. Burnham, LLNL, private communication (1980).

39. F. J. Long and K. W. Sykes, "The Mechanism of the Steam-Carbon Reaction," *Proc. Roy. Soc.,* A193, 377 (1948).

40. H. Y. Sohn and S. K. Kim, "Intrinsic Kinetics of the Reaction Between Oxygen and Carbonaceous Residue in Retorted Oil Shale," *Ind. Eng. Chem. Process Des. Dev.,* 10, 550 (1980).

41. S. A. Steward, LLNL, private communication (1980).

42. G. B. Grebenshchikova, "Study of the Kinetics of the Conversion of Carbon Monoxide by Steam in the Presence of Ash from Lisichansk Coal," *Podzemnaya Gasifikatsiya Uglei*, 2, 54 (1957), translated (1975).
43. A. K. Burnham, *Chemistry of Shale Oil Cracking*, Lawrence Livermore National Laboratory, Report UCRL-84913 for *Proc. A.C.S. Symp. on Oil Shale, Tar Sands and Related Materials*, San Francisco, CA (1980).
44. R. L. Braun and R.C.Y. Chin, *Computer Model for In-Situ Oil Shale Retorting: Effects of Input-Gas Properties*, Lawrence Livermore National Laboratory, Report UCRL-79033 (1977).
45. R. L. Braun, "Results of Computer Simulation of In Situ Oil Shale Retorting," *In Situ*, 3, 173 (1979).
46. J. F. Carley and R. L. Braun, "Ignition of In Situ Oil Shale Retorts with Hot Inert Gas," *In Situ*, 2, (1978).
47. A. E. Lewis and R. L. Braun, "Retorting and Combustion Processes in Surface Oil-Shale Retorts," *Proc. 15th Intersociety Energy Conversion Engineering Conf.*, p. 297, Seattle, WA (1980).
48. O. A. Hougen, K. M. Watson, and R. A. Ragatz, *Chemical Process Principles* (John Wiley & Sons, Inc., New York, NY, 1954).
49. S. S. Tihen, H. C. Carpenter, and H. W. Sohns, "Thermal Conductivity and Thermal Diffusivity of Green River Oil Shale," *Proc. 7th Conf. on Thermal Conductivity*, p. 529 (1958).
50. V. Hlavacek and J. Votruba, "Steady-State Operation of Fixed-Bed Reactors and Monolithic Structures," in *Chemical Reactor Theory, A Review*, L. Lapidus and N. R. Amundson, Eds., (Prentice-Hall, Inc., Englewood Cliffs, NJ, 1977).
51. S. Yagi and D. Kunii, "Studies on Effective Thermal Conductivities in Packed Beds," *AIChE J.* 3, (1957).
52. S. Yagi, D. Kunii and N. Wakao, "Studies on Axial Effective Thermal Conductivities in Packed Beds," *AIChE J.* 6, 543 (1960).
53. J. F. Carley, private communication (1980).
54. C. R. Wilke and C. Y. Lee, "Estimation of Diffusion Coefficients for Gases and Vapors," *Ind. Eng. Chem.*, 47, 1253 (1955).
55. J. O. Hirschfelder, C. F. Curtiss, and R. B. Bird, *Molecular Theory of Gases and Liquids* (John Wiley & Sons, Inc., New York, NY, 1954).
56. C. W. Gear, *Numerical Initial Value Problems in Ordinary Differential Equations* (Prentice-Hall, Inc., Englewood Cliffs, NJ, 1971).

57. L. Lapidus and J. H. Seinfeld, *Numerical Solution of Ordinary Differential Equations* (Academic Press, New York, NY, 1971).

58. P. Henrici, *Discrete Variable Methods in Ordinary Differential Equations* (John Wiley & Sons, Inc., New York, NY, 1962).

59. H. B. Keller, *A New Difference Scheme for Parabolic Problems, Numerical Solution of Partial Differential Equations-II,* SYNSPADE 1970, Hubbard, Ed. (Academic Press, New York, NY, 1971).

60. R.C.Y. Chin and R. L. Braun, "Numerical Solutions of Chemically Reacting Flows in Porous Media," *J. Comp. Phys.*, 34, 74 (1980).

WTF